

Blind, Adaptive, Per Tone Equalization for Multicarrier Receivers

Richard K. Martin and C. Richard Johnson, Jr.¹

School of Electrical & Computer Engineering

Cornell University

Ithaca, NY 14853

e-mail: {frodo,johnson}@ece.cornell.edu

Abstract — This paper proposes the application of traditional blind, adaptive algorithms to the per tone structure for equalization in multicarrier receivers. It is shown that the per tone structure lends itself more readily than the TEQ structure to the application of the Constant Modulus Algorithm (CMA) and Decision-Directed LMS (DD-LMS). The result is that CMA and DD-LMS type algorithms can be derived for the per tone structure, resulting in low-complexity multicarrier equalization algorithms that are both blind and adaptive.

The CM cost function is derived, and the effect of the symbol synchronization on the cost function is explored. Simulations are used to compare the performance of CMA and DD-LMS to the optimal solution (as derived by Van Acker, *et al.*), and to illustrate the situations in which these algorithms excel or falter.

I. INTRODUCTION AND SYSTEM MODEL

Due to the ever-present demand for higher bit rates, researchers are constantly developing new techniques for increasing spectral efficiency. Multicarrier modulation (MCM) is one such technique [1], and its popularity has been increasing steadily. One reason for this is that MCM can easily combat channel dispersion, as long as the cyclic prefix is longer than the channel delay spread.

As a description of the cyclic prefix, consider the baseband model of a typical multicarrier modulation system, as shown in Figure 1. Each block of bits is divided up into N bins, and each bin is viewed as being modulated by a different carrier. An efficient means of implementing the modulation is to use an inverse fast Fourier transform (IFFT). After transmission and reception, an FFT can be used for the demodulation.

In order for the subchannels to be independent, the convolution of the signal and the channel must be a circular convolution. It is actually a linear convolution, so it is made to appear circular by adding a cyclic prefix (CP) to the start of each data block [2], which is obtained by prepending the last ν samples of each block to the beginning of the block. If the channel is shorter than the CP, then the output of each subchannel is equal to the input times a scalar gain factor. The signals in the bins can then be equalized by a bank of complex scalars, referred to as frequency domain equalizers (labeled “FEQs” in Figure 1).

If the CP is not as long as the channel delay spread, then inter-channel interference (ICI) and inter-symbol interference (ISI) will be present, and a channel-shortening (time-domain) equalizer, or TEQ, is needed. The TEQ is chosen such that the convolution of the channel and TEQ has almost all of

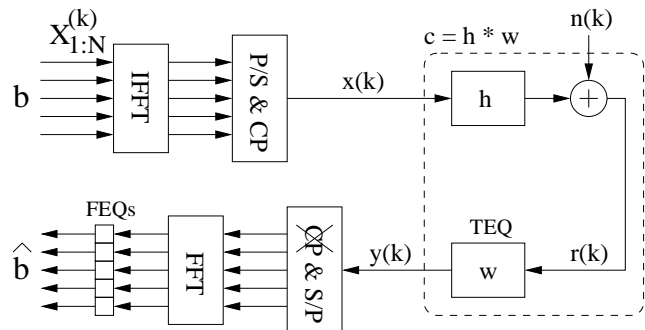


Figure 1: Traditional (TEQ-based) system model. (I)FFT: (inverse) fast Fourier transform, P/S: parallel to serial, CP: add cyclic prefix, xCP: remove cyclic prefix.

its energy in a time window no longer than the CP length. TEQ design (for a *static* environment) has been well explored, notably in [3, 4, 5, 6, 7, 8]. A blind, adaptive equalizer was proposed in [9], but their approach assumes no cyclic prefix; i.e. complete equalization is attempted, rather than channel shortening.

Mathematically, the received signal vector \mathbf{y} is obtained from the transmitted data \mathbf{X} via

$$\underbrace{\begin{bmatrix} y_{ks+\nu-T+2+\delta} \\ \vdots \\ y_{(k+1)s+\delta} \end{bmatrix}}_{\mathbf{y}} = \begin{bmatrix} \mathbf{0}_{(1)} & \mathbf{h} & \cdots & \mathbf{0} \\ \vdots & \ddots & \ddots & \vdots \\ \mathbf{0} & \cdots & \mathbf{h} & \mathbf{0}_{(2)} \end{bmatrix} \cdot \underbrace{\begin{bmatrix} \mathbf{P}\mathcal{I}_N & \mathbf{0} & \mathbf{0} \\ \mathbf{0} & \mathbf{P}\mathcal{I}_N & \mathbf{0} \\ \mathbf{0} & \mathbf{0} & \mathbf{P}\mathcal{I}_N \end{bmatrix}}_{\mathbf{X}} \begin{bmatrix} X_{1:N}^{(k-1)} \\ X_{1:N}^{(k)} \\ X_{1:N}^{(k+1)} \end{bmatrix} + \underbrace{\begin{bmatrix} n_{ks+\nu-T+2+\delta} \\ \vdots \\ n_{(k+1)s+\delta} \end{bmatrix}}_{\mathbf{n}} \quad (1)$$

where \mathbf{h} is a row matrix containing the physical channel, and \mathbf{n} is additive noise or interference. The effective channel \mathbf{H} includes the physical channel \mathbf{h} , the addition of the cyclic prefix (inserted by \mathbf{P}), and the IFFT (implemented by \mathcal{I}_N); and \mathbf{X} contains the symbol of interest as well as the preceding and succeeding symbols. The matrices $\mathbf{0}_{(1,2)}$ are large zero matrices, the sizes of which are determined by the symbol synchronization parameter δ .

Van Acker *et al.* [10] have proposed an alternate equalization structure, called per tone equalization, which accomplishes the same task as the TEQ/FEQ in Figure 1 but with improved performance and comparable complexity. The full details of the per tone structure can be found in [10]. Briefly, demodulation is accomplished by an FFT of size N , which is

¹This work was supported in part by NSF grant ECS-9811297 and NxtWave Communications.

done by premultiplying \mathbf{y} by \mathcal{F}_N . Per tone equalization of bin i is accomplished by forming a linear combination of the i^{th} FFT output and T-1 difference terms of the pre-FFT signal, \mathbf{y} :

$$z_i = \bar{\mathbf{v}}_i^T \cdot \underbrace{\begin{bmatrix} \mathbf{I}_{T-1} & \mathbf{0} & -\mathbf{I}_{T-1} \\ \mathbf{0} & \mathcal{F}_N(i, :) \end{bmatrix}}_{\mathbf{F}_i} \cdot \mathbf{y} \quad (2)$$

The linear combiner (not a tapped delay line) $\bar{\mathbf{v}}_i$ is the equalizer for tone i , and z_i is the equalized data for tone i . The notation in (1) and (2) was introduced in [10], but is repeated here for reference.

Determination of the per tone equalizer coefficients has been explored in [10] and [11]. In [10], the optimal coefficients (in terms of bit rate) are calculated in a least-squares manner, based on knowledge of the transmission channel, and the signal and noise statistics. In [11], the coefficients are determined in a less computationally-intensive fashion through the use of recursive least-squares (RLS), which requires training throughout the adaptation. These approaches are well-suited to a system that has plentiful training and computational power. The proposed algorithms in this paper are designed for situations in which neither condition is true, and in which the environment is modestly time-varying.

This paper is organized as follows. Section II discusses why we are considering the per tone structure instead of the TEQ structure. Section III proposes the per tone CMA (PT-CMA) and per tone DD-LMS (PT-DDLMS) algorithms. The topography of the CM cost function is explored in Section IV. Simulations are given in Section V, and Section VI concludes.

II. CMA FOR A TEQ

One might consider directly adapting the TEQ to minimize the constant modulus cost at the output of the FFT, i.e.

$$J_{CM} = \sum_{i=1}^N \beta_i \mathbb{E} \left[(|Y_i(k)|^2 - \gamma_i)^2 \right], \quad (3)$$

where $Y_i(k)$ is the output of bin i at time k , and where β_i is a weighting coefficient¹. This section briefly discusses why we avoid this approach, and instead investigate blind, adaptive *per tone* equalizers. Consider a stochastic gradient descent of (3).

$$\frac{\partial J_{CM}}{\partial w_l} = 2 \sum_{i=1}^N \beta_i (|Y_i(k)|^2 - \gamma_i) \cdot \frac{\partial (Y_i(k)Y_i^*(k))}{\partial w_l}. \quad (4)$$

The gradient with respect to a complex vector is defined as

$$\frac{\partial (Y_i(k)Y_i^*(k))}{\partial w_l} = \frac{1}{2} \left(\frac{\partial (Y_i(k)Y_i^*(k))}{\partial w_{l,R}} + j \frac{\partial (Y_i(k)Y_i^*(k))}{\partial w_{l,I}} \right) \quad (5)$$

where the subscripts R and I refer to the real and imaginary components, and $*$ denotes complex conjugation. After a modest amount of algebra, this yields

$$\frac{\partial (Y_i(k)Y_i^*(k))}{\partial w_l} = Y_i \left(\sum_{j=1}^N \mathcal{F}_N(i, j) \mathbf{y}(l+j-1) \right)^*, \quad (6)$$

¹If there are different numbers of bits on each subcarrier, then the cost can be weighted in favor of the bins with more bits.

where $\mathbf{y}(j)$ means the j^{th} element of the vector \mathbf{y} , as defined in (1). The resulting stochastic gradient descent algorithm is

$$\mathbf{w}(k+1) = \mathbf{w}(k) - \mu \sum_{i=1}^N \beta_i Y_i (|Y_i(k)|^2 - \gamma_i) \Delta_i^*, \quad (7)$$

where the N different N -vectors Δ_i are obtained by a “sliding FFT,”

$$\begin{bmatrix} \Delta_1^T \\ \vdots \\ \Delta_N^T \end{bmatrix} = \mathcal{F}_N \cdot \begin{bmatrix} \mathbf{y}(1) & \cdots & \mathbf{y}(N) \\ \vdots & & \vdots \\ \mathbf{y}(N) & \cdots & \mathbf{y}(2N-1) \end{bmatrix}. \quad (8)$$

This “sliding FFT” can be implemented efficiently, using little more computational power than a single FFT [10].

There are several problems with this approach. First of all, the sliding FFT adds enough complexity to bring this approach on par with a per tone structure (which ultimately has a higher performance bound), so it makes more sense to pursue per tone CMA. More importantly, the cost (3) will be very large unless all of the FEQs are properly initialized and can successfully track the variation of the channel and the adaptation of the TEQ. The interaction between the adapting TEQ and the adapting FEQ in this regard is difficult to determine explicitly. Instead, we will favor adaptive per tone equalizers, in which the equalizer for each tone absorbs the FEQ for that tone. Readers who prefer the TEQ structure are referred to [12], in which the CM cost and related cost functions are considered for adapting both the TEQ and the carrier frequency estimate.

III. PROPOSED ALGORITHMS

There are many existing algorithms for multicarrier equalization, as discussed in Section I. However, none of the existing solutions for channel shortening or per tone equalization are both blind and adaptive, and most of them are high-complexity. (We exclude [9] here, as it is not applicable to channel shortening in a system with a cyclic prefix.) We propose to use Decision-Directed LMS (DD-LMS) and the Constant Modulus Algorithm (CMA), as applied to the per tone structure, to fill this void.

The DD-LMS algorithm is obtained by performing a stochastic gradient descent of

$$\mathbb{E} [|z_i(k) - Q[z_i(k)]|^2] \quad (9)$$

for each bin i , where $Q[\cdot]$ is the quantization operator (decision device). The resulting algorithm is:

For $i = 1, \dots, N$ and $k = 1, 2, 3, \dots$,

$$\text{DD-LMS: } \begin{cases} z_i(k) = \bar{\mathbf{v}}_i^T(k) \mathbf{F}_i \mathbf{y}(k) \\ e_i(k) = (Q[z_i(k)] - z_i(k)) \\ \bar{\mathbf{v}}_i(k+1) = \bar{\mathbf{v}}_i(k) + \mu e_i(k) \mathbf{F}_i^* \mathbf{y}^*(k). \end{cases} \quad (10)$$

The constant modulus algorithm is a popular alternative to decision-directed algorithms. A detailed review of its convergence behavior in single-carrier systems can be found in [13]. CMA attempts to minimize the dispersion of the equalized symbols by performing a stochastic gradient descent of

$$J_{CM,i} = \mathbb{E} [(|z_i(k)|^2 - \gamma_i)^2] \quad (11)$$

for each bin i . The resulting algorithm is:
For $i = 1, \dots, N$ and $k = 1, 2, 3, \dots$,

$$\text{CMA: } \begin{cases} z_i(k) = \bar{\mathbf{v}}_i^T(k) \mathbf{F}_i \mathbf{y}(k) \\ \bar{\mathbf{v}}_i(k+1) = \bar{\mathbf{v}}_i(k) - \mu z_i(k) (|z_i(k)|^2 - \gamma_i) \mathbf{F}_i^* \mathbf{y}^*(k) \end{cases} \quad (12)$$

Structurally, the only difference between CMA and the DD-LMS algorithm in this application and single-carrier equalization is the presence of the \mathbf{F}_i^* matrices. The computation of $\mathbf{F}_i \mathbf{y}(k)$ is not actually implemented as a matrix-vector multiply. Rather, the last element is obtained directly from the output of the FFT, and the other $T-1$ elements are computed via a single subtraction each (c.f. equation (2)).

A point to emphasize is that these single-carrier techniques and others are readily applicable to the per tone structure, but not as easily to the TEQ/FEQ structure, due to the coupling between the TEQ and FEQs. This is because for per tone equalization, there are no separate FEQs.

IV. TOPOGRAPHY OF THE CM COST SURFACE

This section derives the CM cost function (11) as a function of the equalizer parameters $\bar{\mathbf{v}}_i$ and the symbol synchronization parameter δ , in a fashion similar to that in [13]. Then a low-dimensional example is used to build intuition.

The first step is to decide on appropriate values for the dispersion constants γ_i . Our approach is analogous to the approach taken by Godard [14], i.e. the dispersion constant for tone i will be chosen such that when equalization is achieved, the gradient of the cost function for tone i with respect to the equalizer will be zero. This will lead to dispersion constants that can be independently chosen for each subchannel. The gradient of (11) is

$$\nabla_{\bar{\mathbf{v}}_i} J = \mathbf{E} [4z_i (|z_i|^2 - \gamma_i) \mathbf{F}_i^* \mathbf{y}^*]. \quad (13)$$

To make this zero, we require that

$$\gamma_i \mathbf{E} [z_i \mathbf{F}_i^* \mathbf{y}^*] = \mathbf{E} [z_i |z_i|^2 \mathbf{F}_i^* \mathbf{y}^*]. \quad (14)$$

When equalization has been achieved, we will have $z_i \cong X_i$. We will use this assumption and (1) to get

$$\gamma_i \mathbf{F}_i^* \mathbf{H}^* \mathbf{E} [X_i \mathbf{X}^*] = \mathbf{F}_i^* \mathbf{H}^* \mathbf{E} [X_i |X_i|^2 \mathbf{X}^*]. \quad (15)$$

Denote the vector \mathbf{e}_j as the vector of all zeros except for a 1 in position j . Assuming that the input data is uncorrelated between symbols and between tones, (15) becomes

$$\gamma_i \mathbf{F}_i^* \mathbf{H}^* \mathbf{E} [|X_i|^2] \mathbf{e}_{N+i} = \mathbf{F}_i^* \mathbf{H}^* \mathbf{E} [|X_i|^4] \mathbf{e}_{N+i}. \quad (16)$$

Thus, an appropriate choice for γ_i is

$$\gamma_i = \frac{\mathbf{E} [|X_i|^4]}{\mathbf{E} [|X_i|^2]} \quad (17)$$

This was to be expected, since it closely matches Godard's choice. The difference is that we are now free to assign different statistics to each subchannel. This is necessary for transmission schemes that use bit loading (such as DSL), since $\mathbf{E} [|X_i|^4]$ will generally vary with the bin number i , even if the power $\mathbf{E} [|X_i|^2]$ is held constant.

Now we can discuss the CM cost function. Recall that $\mathbf{y} = \mathbf{H}\mathbf{X} + \mathbf{n}$ and $z_i = \bar{\mathbf{v}}_i^T \mathbf{F}_i \mathbf{y}$. Thus,

$$\begin{aligned} z_i &= \left(\mathbf{H}^T \mathbf{F}_i^T \bar{\mathbf{v}}_i \right)^T \mathbf{X} + \left(\mathbf{F}_i^T \bar{\mathbf{v}}_i \right)^T \mathbf{n} \\ &\triangleq \sum_j c_j X_j + \sum_j f_j n_j. \end{aligned} \quad (18)$$

In the definitions of \mathbf{c} and \mathbf{f} , the subscript i has been dropped for simplicity. We will make use of these definitions momentarily.

We can expand (11) to

$$J_{CM,i} = \mathbf{E} (|z_i|^4) - 2\gamma_i \mathbf{E} (|z_i|^2) + \gamma_i^2, \quad (19)$$

which requires a calculation of $\mathbf{E} (|z_i|^4)$ and $\mathbf{E} (|z_i|^2)$. Assuming that the noise and the data are uncorrelated and the noise is stationary,

$$\mathbf{E} (|z_i|^2) = \sum_k \mathbf{E} [|X_k|^2] \cdot |c_k|^2 + \sigma_n^2 \sum_k |f_k|^2. \quad (20)$$

Determining $\mathbf{E} (|z_i|^4)$ is more complicated.

$$\begin{aligned} \mathbf{E} (|z_i|^4) &= \mathbf{E} \left(\sum_k c_k X_k + \sum_a f_a n_a \right) \left(\sum_l c_l X_l + \sum_b f_b n_b \right) \\ &\quad \left(\sum_{\hat{i}} c_{\hat{i}}^* X_{\hat{i}}^* + \sum_c f_c^* n_c^* \right) \left(\sum_j c_j^* X_j^* + \sum_d f_d^* n_d^* \right) \end{aligned} \quad (21)$$

(The hat on the i is used to distinguish the summation index \hat{i} from the tone index i .) This will produce 16 cross-terms. The first cross-term corresponds to the noiseless case, and the last term will have a similar structure. The 8 cross-terms with an odd number of noise factors drop out. Of the remaining 6 terms, two are such that the signal and noise are paired with their unconjugated counterparts, so they also drop out (assuming that the source is QAM, as in DSL or IEEE 802.11a); and the remaining four of these terms are identical. After an extensive amount of algebra, we arrive at the following general form of the CM cost function,

$$\begin{aligned} J_{CM,i} &= \sum_k [\mathbf{E} (|X_k|^4) - 2\mathbf{E}^2 (|X_k|^2)] \cdot |c_k|^4 \\ &+ 2 \left[\sum_k \mathbf{E} (|X_k|^2) \cdot |c_k|^2 \right]^2 - 2 \frac{\mathbf{E} [|X_i|^4]}{\mathbf{E} [|X_i|^2]} \sum_k \mathbf{E} (|X_k|^2) \cdot |c_k|^2 \\ &+ \left(\frac{\mathbf{E} [|X_i|^4]}{\mathbf{E} [|X_i|^2]} \right)^2 + 4 \left(\sum_k \mathbf{E} [|X_k|^2] \cdot |c_k|^2 \right) \left(\sigma_n^2 \sum_k \mathbf{E} |f_k|^2 \right) \\ &+ [\mathbf{E} (|n_k|^4) - 2\sigma_n^4] \sum_k |f_k|^4 + 2 \left[\sigma_n^2 \sum_k \mathbf{E} |f_k|^2 \right]^2 \\ &- 2 \frac{\mathbf{E} [|X_i|^4]}{\mathbf{E} [|X_i|^2]} \sigma_n^2 \sum_k \mathbf{E} |f_k|^2 \end{aligned} \quad (22)$$

The subscripts on X are all tone indices, and the subscripts on c and f are tap indices. If we were to remove these tone subscripts on X , this would simplify (22) to the result in equation (61) in the appendix of [13]. Alternatively, (22) could be simplified by assuming that at least the power $\mathbf{E} [|X_k|^2]$ does

not vary with the bin index k . That is valid in most applications. However, [15] and [16] have shown that if the transmit power is optimized across the bins, then slight performance gains can be achieved, so that assumption does entail a loss of generality.

The most important conclusion we can reach from our analysis of the CMA cost function is that its similarity with the traditional CM cost function in [13] suggests a similarity of behavior. Furthermore, the inputs to the IFFT are generally white (across both symbols and frequency bins), which is analogous to the assumption made in most single-carrier CMA papers, in which the source symbols are assumed to be white. The full details are not treated here, but assuming the appropriate assumptions are verified for the multicarrier case (corresponding to the assumptions made in the single carrier case), *mutatis mutandis*, the rich literature for single-carrier CMA can be applied here. In particular, we cannot obtain a closed form solution for the locations of the global minima.

In order to view this cost function, we consider low-order examples. Figure 2 shows the CM cost function (and the amalgamated MSE, which is a composition of the MSE's for different delays [13]) for tone 2 (the plots for tone 1 are similar). The variables were: a 3-tap channel, a cyclic prefix length of $\nu = 1$, and a 2-tap equalizer on each of the 2 tones. The three plots represent different values of the symbol synchronization, and the axes on each of the plots represent the equalizer taps for tone 2. The CM cost function is periodic in δ , with period $N + \nu = 3$ in this case (hence only three plots are needed).

Figure 2 provides intuition regarding the effects of the symbol synchronization. It is clear that the parameter δ drastically changes the shape of the cost surface, the depth of the minima, and even the number of minima. For this reason, it is expected that the performance of per tone CMA will vary significantly with δ , so symbol synchronization must be done with care. However, if $N = 8196$, as in the European HDTV standard [17], there might be a more gradual transition between the cost surfaces as δ varies, and we must be cautious when generalizing from such a low order example.

V. SIMULATIONS

The toy problem in Section IV is useful for gaining intuition, but a practical study requires much larger dimensions. For the following simulations the parameters were chosen to approximately match those in the IEEE 802.11a standard [18], though this was done to provide a realistic set of parameters rather than to focus on that particular application. Specifically, we used an FFT size of $N = 64$, 12 null carriers, a CP length of $\nu = 16$, an equalizer of $T = 16$ taps per tone, and an SNR of 40 dB (noise was modeled as AWGN).

Figure 3 shows the SNR obtained at the output of the receiver for tone 2 (the first tone that is not a null carrier), with the symbol synchronization on the horizontal axis. The dashed line is the SNR of the equalizer settings determined in Section V.A in [10], the dotted line is the SNR at initialization (corresponding to no equalizer), and the solid line is the SNR of the CMA settings after convergence. The poor performance for $-40 \leq \delta \leq 0$ is not of importance because those values of δ corresponding to picking a symbol synchronization such that each received block is a significant mixture of *two* transmitted blocks, i.e. such values of δ would not be used in any practical system. Figure 4 shows similar plots, but for the CM cost rather than the SNR, and the same comments apply.

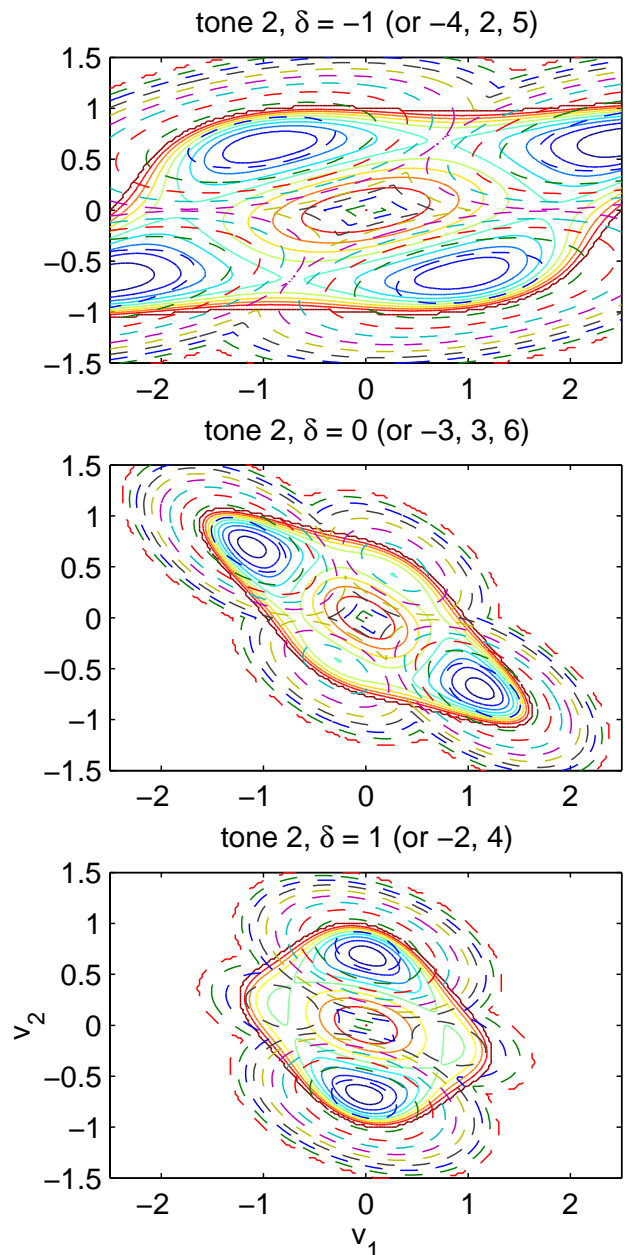


Figure 2: The CM (solid) and amalgamated MSE (dashed) cost functions as a function of equalizer taps (v_1, v_2) and symbol synchronization (δ).

There are several features to note from these results. First, for a reasonable range of values of δ around the optimal value, the performance of per tone equalizers is relatively insensitive to the choice of δ (in our example, this is the region $4 \leq \delta \leq 16$ or $4 \leq \delta \leq 35$, depending on how much variation in the SNR is considered acceptable). Second, note that the performance of CMA (after convergence) closely matches the performance of [10], especially for the “good” choices of δ . Also note that the performance is periodic in δ , with period equal to the symbol size $s = N + \nu = 64 + 16 = 80$.

Figure 5 shows the SNR for tone 2 as a function of time. The symbol synchronization parameter δ was chosen to be within the range discussed above, i.e. $\delta = 12$. Observe that

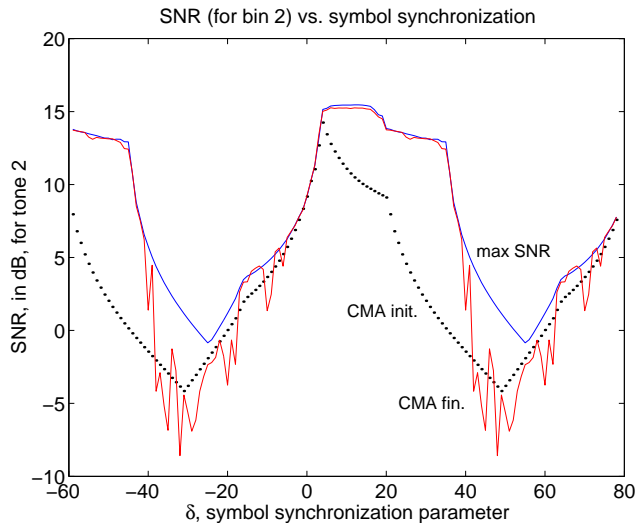


Figure 3: SNR for CMA and the optimal MMSE solution as a function of symbol synchronization.

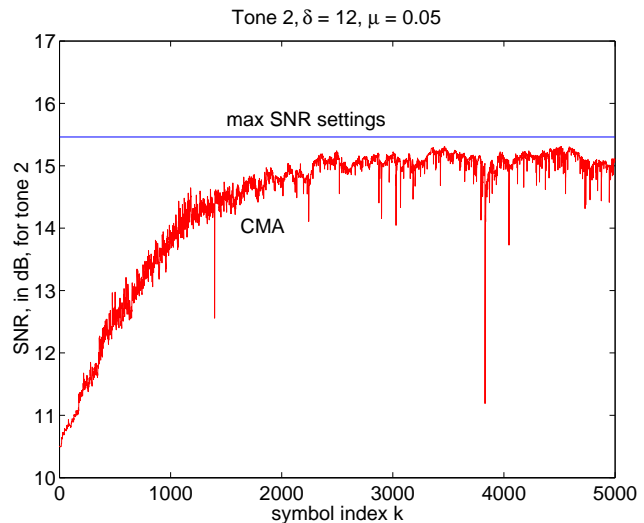


Figure 5: SNR (for tone 2) over time, using CMA.

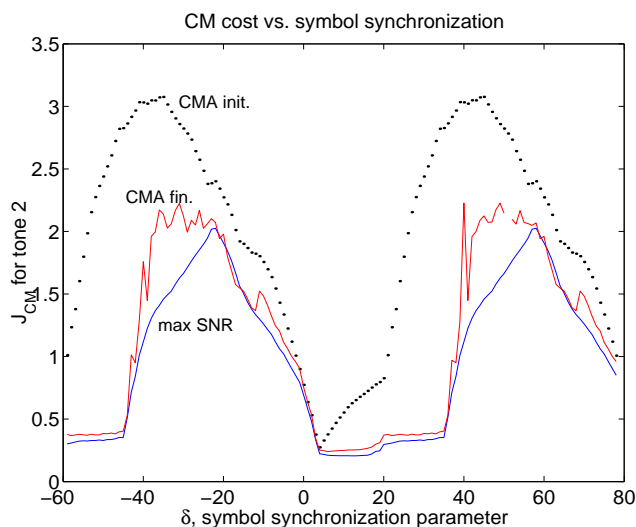


Figure 4: CM cost for CMA and the optimal MMSE solution as a function of symbol synchronization.

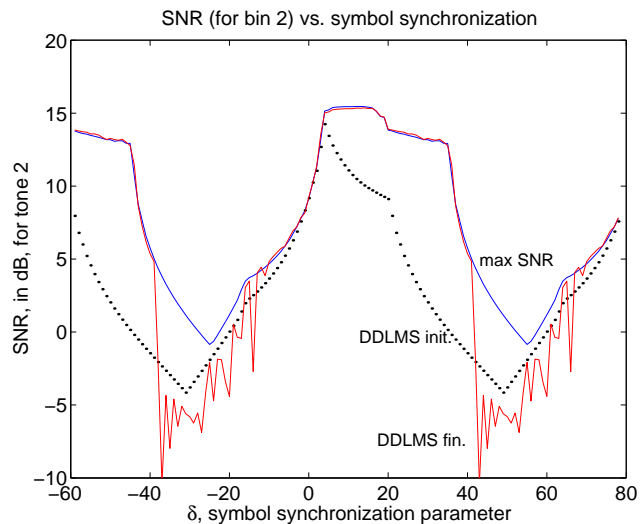


Figure 6: SNR for DD-LMS and the optimal MMSE solution as a function of symbol synchronization.

most of the convergence takes place within 1000 symbols, and optimal performance is achieved asymptotically.

Figure 6 and Figure 7 show the same simulation, but performed using DD-LMS as the adaptive algorithm. A different step size was used for DD-LMS than for CMA under the same conditions. In each case, the stepsize was chosen to be as large as possible without significant asymptotic performance degradation. Observe that DD-LMS exhibits better convergence speed.

One might ask why DD-LMS would not always be favored over CMA. Conventional wisdom states that DD-LMS can only converge to a good answer if the initial decisions are fairly accurate. If the channel is severe enough, this may not be the case. In such a situation, CMA should be used for the first stage of adaptation, then a switch should be made to DD-LMS [19].

VI. CONCLUSIONS

We have proposed the use of “traditional” blind, adaptive algorithms for use in per tone equalization for multicarrier receivers. A theoretical treatment of the CM cost function has been provided, and the feasibility of CMA and DD-LMS has been shown via simulations. We have demonstrated that the asymptotic performance of CMA and DD-LMS approaches that of Van Acker’s solution, and that near-optimal performance can be achieved within 10 to 100 symbols per equalizer tap.

REFERENCES

- [1] J. A. C. Bingham, “Multicarrier Modulation for Data Transmission: An Idea Whose Time Has Come,” *IEEE Communications Magazine*, vol. 28, no. 5, pp. 5–14, May 1990.
- [2] A. Peled and A. Ruiz, “Frequency Domain Data Transmission Using Reduced Computational Complexity Algorithms,” in *The proceedings of the 1980 International Conference on Acoustics*,

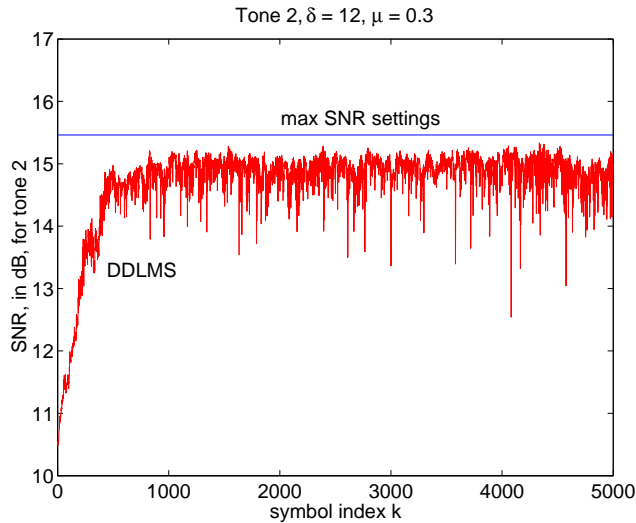


Figure 7: SNR (for tone 2) over time, using DD-LMS.

Speech, and Signal Processing, Denver, Colorado, Apr. 1980, pp. 964–967.

- [3] J. S. Chow, J. M. Cioffi, and J. A. C. Bingham, “Equalizer Training Algorithms for Multicarrier Modulation Systems,” in *IEEE International Conference on Comm.*, May 1993, pp. 761–765.
- [4] P. J. W. Melsa, R. C. Younce, and C. E. Rohrs, “Impulse Response Shortening for Discrete Multitone Transceivers,” *IEEE Trans. on Comm.*, vol. 44, pp. 1662–1672, Dec. 1996.
- [5] G. Arslan, B. L. Evans, and S. Kiaei, “Equalization for Discrete Multitone Receivers To Maximize Bit Rate,” *IEEE Trans. on Signal Processing*, vol. 49, no. 12, pp. 3123–3135, Dec. 2001.
- [6] B. Farhang-Boroujeny and M. Ding, “Design Methods for Time-Domain Equalizers in DMT Transceivers,” *IEEE Trans. on Comm.*, vol. 49, no. 3, pp. 554–562, Mar. 2001.
- [7] W. Henkel and T. Kessler, “Maximizing the Channel Capacity of Multicarrier Transmission by Suitable Adaptation of the Time-domain Equalizer,” *IEEE Trans. on Comm.*, vol. 48, no. 12, pp. 2000–2004, Dec. 2000.
- [8] N. Lashkarian and S. Kiaei, “Optimum Equalization of Multicarrier Systems: A Unified Geometric Approach,” *IEEE Trans. on Comm.*, vol. 49, pp. 1762–1769, Oct. 2001.
- [9] M. de Courville, P. Duhamel, P. Madec, and J. Palicot, “Blind equalization of OFDM systems based on the minimization of a quadratic criterion,” in *Proceedings of the Int. Conf. on Communications*, Dallas, TX, June 1996, pp. 1318–1321.
- [10] K. Van Acker, G. Leus, M. Moonen, O. van de Wiel, and T. Pollet, “Per Tone Equalization for DMT-Based Systems,” *IEEE Trans. on Comm.*, vol. 49, no. 1, pp. 109–119, Jan. 2001.
- [11] K. Van Acker, G. Leus, M. Moonen, and T. Pollet, “RLS-based initialization for per tone equalizers in DMT-receivers,” in *Proceedings of the European Signal Processing Conference (Eusipco 2000)*, Tampere, Finland, Sept. 2000.
- [12] W. Chung and C. R. Johnson, Jr., “Blind, Adaptive Carrier Frequency Offset Correction for Multicarrier Systems,” in *Proceedings of the 2002 Conference on Information Sciences and Systems*, Princeton, NJ, Mar. 2002.
- [13] C. R. Johnson, Jr., P. Schniter, T. J. Endres, J. D. Behm, D. R. Brown, and R. A. Casas, “Blind Equalization Using the Constant Modulus Criterion: A Review,” *Proceedings of the IEEE*, vol. 86, pp. 1927–1950, Oct. 1998.
- [14] D. N. Godard, “Self-Recovering Equalization and Carrier Tracking in Two-Dimensional Data Communication Systems,” *IEEE Trans. on Comm.*, vol. COM-28, pp. 1867–1875, Nov. 1980.
- [15] N. Al-Dhahir and J. M. Cioffi, “Bandwidth optimization for combined equalization and coding transceivers with emphasis on the MMSE-DFE,” *IEEE Milcom*, vol. 2, pp. 471–475, Oct. 1993.
- [16] P. Chow, *Bandwidth optimized digital transmission techniques for spectrally shaped channels with impulse noise*, Ph.D. thesis, Stanford University, 1993.
- [17] The European Telecommunications Standards Institute, “Digital Video Broadcasting (DVB); Framing Structure, Channel Coding and Modulation for Digital Terrestrial Television. ETSI EN 300 744 V1.4.1,” 2001 Edition.
- [18] The Institute of Electrical and Electronics Engineers, “Wireless LAN Medium Access Control (MAC) and Physical Layer (PHY) Specifications. IEEE Std. 802.11a,” 1999 Edition.
- [19] J. R. Treichler, M. G. Larimore, and J. C. Harp, “Practical Blind Demodulators for High-Order QAM Signals,” *Proceedings of the IEEE*, vol. 86, pp. 1907–1926, Oct. 1998.